Indian Journal of Chemistry
Vol. 60A, March 2021, pp. 370-377

# A DFT study on electronic excitations, charge transfer and NLO properties of visible absorbing squaraine and thiosquaraine dyes

Prabhakar Chetti[a,]*, Anuj Tripathi[a], Ritu Mittal[a] & Atul Chaskar[b]

[a]Department of Chemistry, National Institute of Technology, Kurukshetra 136 119, India
[b]National Centre for Nanosciences and Nanotechnology, University of Mumbai, Mumbai 400 098, India

*E-mail: chetty_prabhakar@yahoo.com

*Received 10 May 2020; revised and accepted 29 January 2021*

Density functional calculations have been performed to see the effect of sulfur substitution in place of oxygen at central four membered acceptor squarate ring on electronic excitations, charge transfer and second order non-linear optical properties in visible absorbing squaraines (SQ). Molecules oxy-thiosquaraines (OSQ) and thiosquaraines (SSQ) have shown red shift in absorption as compared to their corresponding SQ molecules. The lowest five electronic excitations for all the molecules have been calculated by using TDDFT method. Further, effect of electron donating and electron withdrawing groups on absorption maxima have been studied. The large red shifts in case of electron withdrawing group within the same series of molecules (SQ, OSQ and SSQ) are due to destabilization of HOMO and stabilization of LUMO levels. Charge transfers in these molecules are reported by using VMOdes. Second hyperpolarizabilities (⟨γ⟩) for these molecules are calculated by SOS method. This study may be helpful in synthesizing new C-N bonding SQ, OSQ and SSQ dyes which are further useful in NLO applications.

**Keywords:** Squaraines, Thiosquaraine, Oxy-thiosquaraines, Second hyperpolarizabilities, Diradicaloid character

Squaraine dyes are an important class of organic functional molecules and are synthesized from squaric acid, i.e., 1,2-dihydroxycyclobutene-3,4-dione condensed with heterocyclic or aromatic components. These bis-substituted derivatives of squaric acid are of two types viz., 1,2-bis and 1,3-bis donor substituted derivatives (Scheme 1). The former dyes don't have distinctive properties and they are essentially of merocyanines, whereas the later dyes are having a unique type of chromophore which is neither cyanine nor merocyanine and has exceptional characteristics of light absorption and are generally called as squaraines or squarylium dyes.

The synthesis of squaraines was first reported by Treibs and Jacob in 1965[1] and involves the condensation of squaric acid with two equivalents of electron-rich aromatics such as unsubstituted pyrroles and 1,3,5-trihydroxybenzene under acidic conditions. Later on, many squaraine dyes has been reported with different aromatic or heterocyclic components[2-6]. Aniline based squaraines were described for the first time in 1966 by Sprenger and Ziegenbein[7]. The treatment of squaric acid with two molar equivalents of amines results in the formation of symmetrical squaraines commonly referred to as aminosquaraines[8].

Squaraine dyes normally shows sharp and intense absorption in the solution state from visible to near infrared (NIR) region depending on the strength of donor at 1,3-positions of the squarate ring. If the donor group at 1,3-positions of squarate ring is bonded with nitrogen atom (C-N bonding molecules, shown in Scheme 2a), the absorption is in the visible

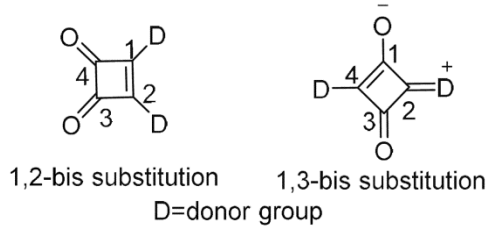


Scheme 1 — Schematic representation for 1,2 and 1,3-bis donor substituted derivatives of squaric acid

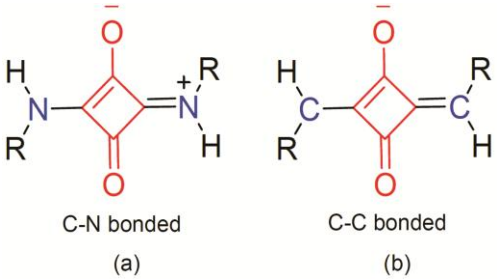


Scheme 2 — Schematic representation for (a) C-N bonding and (b) C-C bonding squaraines

region[9-14] from 300-500 nm with molar extinction coefficient $\geq 10^4$ $cm^{-1}$ $M^{-1}$ while the ring is bonded with carbon atom (C-C bonding molecules, shown in Scheme 2b), then the absorption is in the range of 600-900 nm (visible-NIR region) with molar extinction[4-6, 15-21] coefficient $\geq 10^5$ $cm^{-1}$ $M^{-1}$. This feature contributes greatly to the development of optoelectronic materials and devices of modern times that are useful for high technology applications[22-29].

Conventionally, squaraine dyes are known as donor–acceptor–donor (D-A-D) dyes and believed that the strength of donor (substituent side groups) and acceptor (four-membered ring and the carbonyl oxygens), will influence the absorption maxima[4, 30-34]. In our earlier reports based on the Symmetry Adopted Cluster Configuration Interaction (SAC-CI) calculations on C-C bonding squaraines, it is shown that charge transfer from donor to the acceptor is minimal[10, 13-14, 35-37]. The magnitude of charge transfer in the case of C-C bonding squaraines is small and showed biradical character[35-37] whereas C-N bonding squaraines are purely charge transfer kind of molecules[10, 13-14]. However, in both the cases the major transition is from highest occupied molecular orbital (HOMO) to the lowest unoccupied molecular orbital (LUMO) and is mainly localized at the acceptor[10, 35-37]. A detailed comparison between C-C and C-N bonding squaraines have been made using quantum mechanical calculations, and showed that both C-C and C-N bonding squaraines are of D-A-D type molecules where charge transfer take place from both oxygen of central squarate ring and donor groups to the central four-member acceptor ring (squarate). The large red shift in case of C-C bonding squaraines compared to corresponding C-N bonding squaraines is due to extended π-backbone along with presence of diradicaloid character[13-14].

In the present study, we are interested to see the effect of core substitution on central four membered squarate ring with sulfur in place of oxygen (oxy-thiosquaraines obtained by replacing one of the two carbonyl oxygens of central four membered ring with sulfur and thiosquaraines, obtained by replacing both carbonyl oxygens with sulfur to their parent squaraine molecule). An in-depth analysis of the nature of transitions and charge transfer characteristics in visible absorbing (C-N bonding) squaraines (SQ), oxy-thiosquaraines (OSQ) and thiosquaraines (SSQ) (Scheme 3) and their response towards the second-hyperpolarizabilities have been made.

## Computational Methodology

The ground state energy minimization of all the molecules in its stable configurations have been performed using the Berny optimization algorithm at the DFT-B3LYP in conjunction with the *6-311+G(d,p)* basis set[38-39] without any symmetry constraints. The obtained geometries were then subjected to vibrational frequencies at the same level and found to be minima on the potential energy surface characterized by the real values for frequencies. The triplet state energy minimizations were performed for the lowest energy configuration at the same level of theory to estimate the diradicaloid character based on the singlet-triplet energy gap.

The vertical electronic spectra and the corresponding five lowest singlet energy transitions have been predicted and analyzed for the lowest energy configuration using the time-dependent density functional theory (TDDFT) at B3LYP/6-311+G(d,p) level. The electron densities in the frontier molecular orbitals have been analyzed using the Mulliken population technique at the same level of theory. All the calculations were carried out using Gaussian 16W software[40].

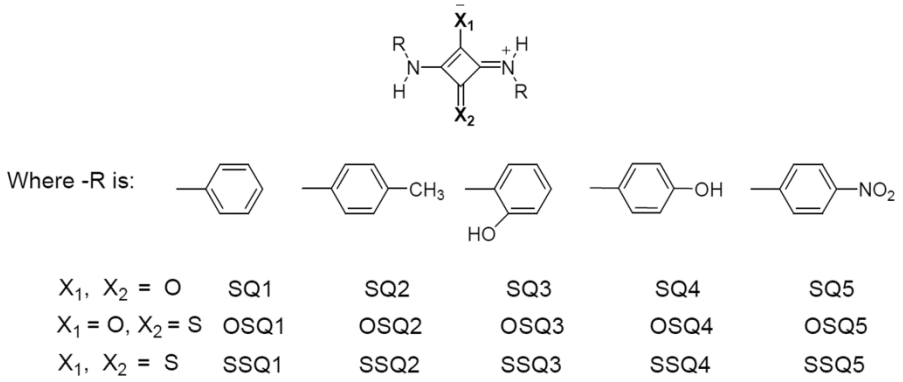


Scheme 3 — Schematic representation for Structures of the molecules considered in this study

The three-term model[10] (including the ground state, lowest excited state, and the dominant higher-lying excited state) has been applied to obtain the average static third-order polarizabilities, ⟨γ⟩ in the context of the Sum-Over-States approach[41].

As the NLO properties are found to be affected by the electronic transitions, the ⟨γ⟩ values were calculated using the electronic transition energies obtained at various DFT functionals namely B3LYP, BH and HLYP, PBE0, M06, M06-2X, CAM-B3LYP and ωB97XD, in conjunction with 6-311+G(d,p) basis set.

## Results and Discussion

### Geometry and structure

The SQ and SSQ molecules exists in two possible configurations, **a** and **b** (syn and anti-arrangement of R-groups) as shown in Scheme 4a and the corresponding molecules are designated as SQ-a and SQ-b; SSQ-a and SSQ-b. For OSQ, three possible configurations '**a**', '**b**' and '**c**' exists stable on potential energy surface (anti-arrangement, syn-arrangement towards sulfur and oxygen atoms of R-groups, respectively) as shown in Scheme 4b and the corresponding molecules are designated as OSQ-a, OSQ-b and OSQ-c. The geometry optimizations of all the molecules in these configurations with different R-groups have been performed at the DFT level as discussed above. The relative energies of stable configurations for all the molecules are presented in Table 1. From the table, it is observed that, for SQ and SSQ series, configuration '**a**' is relatively more stable than configuration '**b**' by ~0.38-0.88 kcal/mol and ~2.35-2.91 kcal/mol, respectively. For OSQ series, configuration '**c**' is relatively more stable than '**a**' and '**b**' by 0.16-2.61 kcal/mol and 8.99-10.66 kcal/mol, respectively. Henceforth, the energetically stable configuration for each of the molecule in the series is considered for all successive calculations. The optimized structures along with their relative energies of all the isomers considered for the study are shown in Supplementary Data, Table S1.

### Electronic excitations

In order to access the density functionals and to obtain the benchmark method, the absorption energies for SQ set of molecules have been calculated with various functionals and compared with their experimental values which are presented in Supplementary Data, Table S2. The data infers that the calculated values are underestimated by 0 to 4.2%, 1.5 to 5.5%, 2.9 to 6.9 %, 6.8 to 13.9%, 2.9 to 16.5%, 6.6 to 13.4% and 7.3 to14.7% for B3LYP, M06, PBE0, M06-2X, BHandHLYP, CAM-B3LYP and ωB97XD methods, respectively. The small error of B3LYP compared to other functional indeed suggests that it can be considered as the benchmark method and therefore used to obtain the absorption wavelengths for the OSQ and SSQ set of molecules.

Accessing the effect of substitution by the electron donating/withdrawing groups on the phenyl ring of the donor, it is observed that the electron-donating methyl and hydroxyl groups on the phenyl ring as in SQ2 and SQ3; change in the position of the hydroxyl group on the phenyl ring as in SQ4 as well has no significant impact on the absorption maxima as seen from the very small red-shift (4-22 nm) as compared to the unsubstituted molecule SQ1. However, substitution with the electron-withdrawing nitro group as in SQ5 has greater contribution and have red-shifted the absorption maximum around 60 nm with respect to SQ1 indicated that the charge transfer is more from donor to acceptor. The normalized absorption spectra of the molecules in each series i.e.

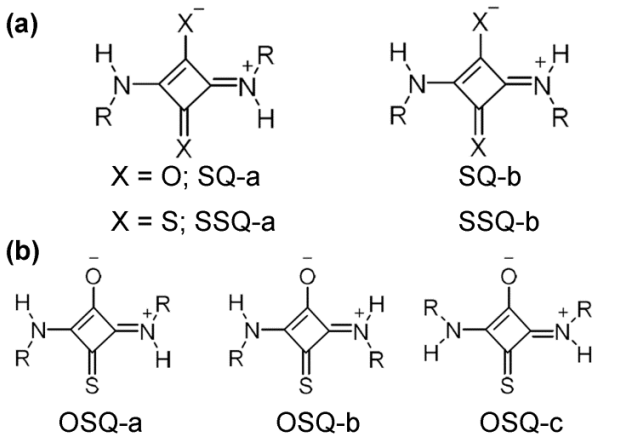


Scheme 4 — Schematic representation for (a) Two stable geometrical configurations of SQ and SSQ and (b) Possible geometrical configurations of OSQ

Table1 — Relative energies (RE in kcal/mol) of SQ, OSQ, SSQ molecules

| Conformation ↓ | 1 | 2 | 3 | 4 | 5 |
|---|---|---|---|---|---|
| SQ | | | | | |
| SQ-a | 0.00 | 0.00 | 0.00 | 0.00 | 0.00 |
| SQ-b | 0.82 | 0.79 | 0.38 | 0.83 | 0.88 |
| OSQ | | | | | |
| OSQ-a | 2.61 | 2.55 | 0.16 | 2.58 | 2.43 |
| OSQ-b | 9.11 | 9.01 | 10.66 | 8.99 | 9.03 |
| OSQ-c | 0.00 | 0.00 | 0.00 | 0.00 | 0.00 |
| SSQ | | | | | |
| SSQ-a | 0.00 | 0.00 | 0.00 | 0.00 | 0.00 |
| SSQ-b | 2.91 | 2.84 | 2.47 | 2.35 | 2.80 |

SQ, OSQ and SSQ are shown in Fig. 1a-c. However, in any case, the electronic transition corresponding to the absorption maximum is due to the transition from HOMO to LUMO, shown in the Table 2.

**Effect of sulfur on electronic excitations**

The substitution of oxygen atoms in the acceptor ring by sulfur atoms as in OSQ and SSQ showed interesting results on the absorption properties. The calculated absorption wavelengths are presented in Table 2. By replacing oxygen with sulfur substituent to the central ring increases the absorption maximum. Molecule OSQ1 shows ~40 nm red-shift while SSQ1 shows ~65 nm red-shift in absorption as compared to SQ1 (shown in Fig. 2). Similar results are observed for OSQ2 and SSQ2 as the absorption maxima at 421 nm and 436 nm, are red-shifted by 30 nm and 56 nm, respectively, than that of SQ2. The same trend is observed for ortho substituted hydroxyl group at phenyl ring. The calculated absorption for OSQ3 and SSQ3 are 434 nm and 450 nm, respectively (shows red shift of 48 nm and 64 nm, respectively, Fig. S1, Supplementary Data). There is an increase in absorption towards longer wavelength region is noticed as moving from SQ4→OSQ4→SSQ4 (399 nm→419 nm →433 nm). Further, introduction of nitro group at para position to the phenyl ring shows larger red-shift in OSQ as well as in SSQ. OSQ5 is having absorption maximum at 498 nm and that of SSQ5 is at 526 nm, which indicate larger red shift of 50 nm and 78 nm, respectively, from SQ5 molecule. The decreasing order of absorption for all the studied molecules is: SSQ> OSQ>SQ when compared with same substituents on central ring (Table 2). This result was attributed due to the greater donor ability of sulfur in comparison to the oxygen. Overall, it is concluded that the red-shifted absorptions are due to the greater donor ability and larger atomic size of sulfur in comparison with oxygen atom[42].

Table 2 — Absorption maxima ($\lambda_{cal}$ in nm), oscillator strength (*f*), major transitions (MT) and % Ci coefficient for all the molecules calculated at TD-B3LYP/6-311+G(d,p) level of theory for B3LYP/ 6-311+G (d,p) optimized geometries

| Name | $\lambda_{exp}$ | $\lambda_{cal}$ | *f* | MT | %Ci |
|---|---|---|---|---|---|
| SQ1 | 399[a,b] | 386 | 0.936 | H→L | 99 |
| SQ2 | 406[a,b] | 390 | 1.073 | H→L | 99 |
| SQ3 | 403[a] | 386 | 0.913 | H→L | 96 |
| SQ4 | 408[a,b] | 408 | 0.657 | H→L | 98 |
| SQ5 | 454[b] | 448 | 1.019 | H→L | 99 |
| OSQ1 | -- | 423 | 0.419 | H→L | 96 |
| OSQ2 | -- | 421 | 0.514 | H→L | 97 |
| OSQ3 | -- | 434 | 0.456 | H→L | 96 |
| OSQ4 | -- | 419 | 0.560 | H→L | 96 |
| OSQ5 | -- | 498 | 0.458 | H→L | 98 |
| SSQ1 | -- | 440 | 0.330 | H→L | 68 |
| | | | | H→L+1 | 28 |
| SSQ2 | -- | 436 | 0.419 | H→L | 57 |
| | | | | H→L+1 | 40 |
| SSQ3 | -- | 453 | 0.389 | H→L | 86 |
| | | | | H→L+1 | 11 |
| SSQ4 | -- | 433 | 0.459 | H→L | 52 |
| | | | | H→L+1 | 44 |
| SSQ5 | -- | 526 | 0.377 | H→L | 98 |

[a]Reference 10, [b]Reference 46

**Frontier molecular orbitals**

For deeper understanding of energy levels in these molecules, frontier molecular orbitals are generated and are shown in Table 3 for SQ1, OSQ1 and SSQ1 and the orbital energies are shown in Table 4 (molecular orbital pictures of rest of the molecules are

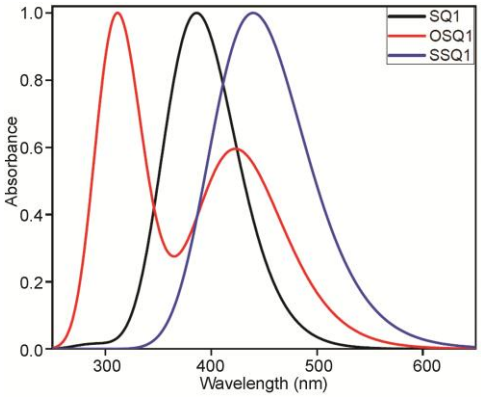


Fig. 2 — Comparative absorption spectra of SQ1, OSQ1, and SSQ1 molecules

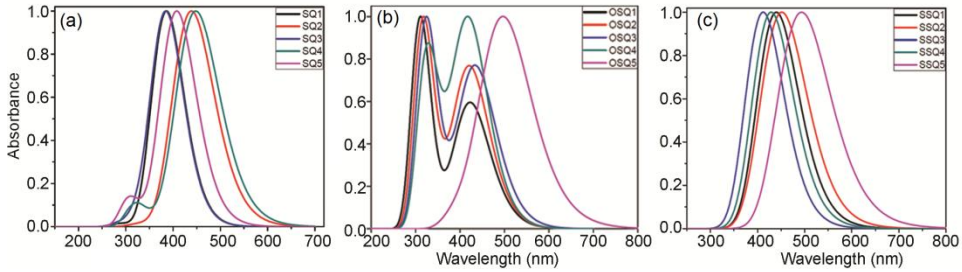


Fig. 1 — Electronic absorption spectra of (a) SQ1-SQ5, (b) OSQ1-OSQ5 and (c) SSQ1-SSQ5 molecules

Table 3 — Molecular orbitals pictures of HOMO-LUMO

| Name | HOMO | LUMO |
|---|---|---|
| SQ1 | 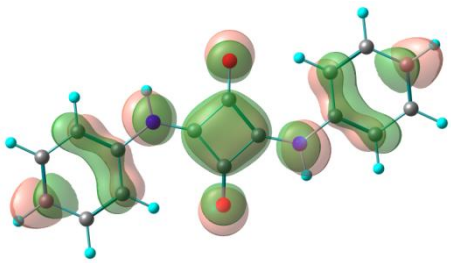 | 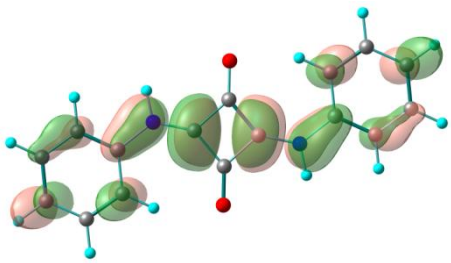 |
| OSQ1 | 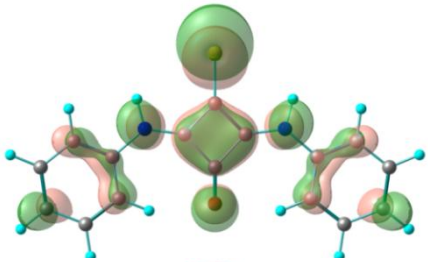 | 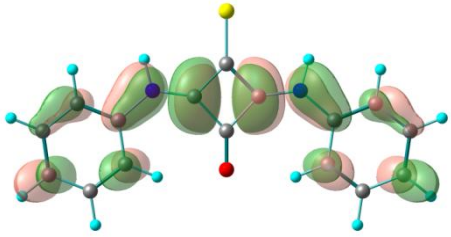 |
| SSQ1 | 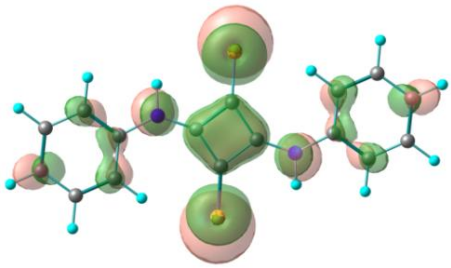 | 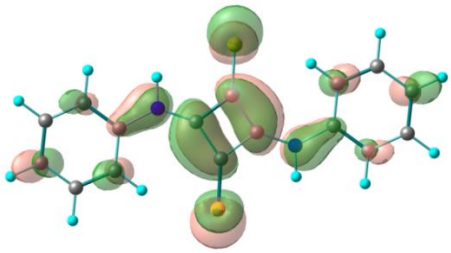 |

Table 4 — Calculated HOMO, LUMO energies and H-L gap (in eV), singlet-triplet gap ($\Delta E_{S-T}$ in kcal/mol) and second hyperpolarizabilities ($\gamma$ in esu) obtained for the B3LYP/6-311+G(d,p) optimized geometries of the molecules

| Molecule | HOMO | LUMO | H-L gap | $E_{S-T}$ | $\gamma_{cal}\times10^{-34}$ |
|---|---|---|---|---|---|
| SQ1 | -5.72 | -2.31 | 3.41 | 44.7 | -2.0 (-0.53)[a] |
| SQ2 | -5.55 | -2.17 | 3.38 | 43.1 | -2.8 (-0.55)[a] |
| SQ3 | -5.76 | -2.31 | 3.45 | 43.8 | -2.0 (-0.12)[a] |
| SQ4 | -5.72 | -2.43 | 3.29 | 42.7 | -1.4 |
| SQ5 | -6.62 | -3.59 | 3.03 | 42.1 | -5.2 |
| OSQ1 | -5.68 | -2.41 | 3.27 | 44.6 | -0.6 |
| OSQ2 | -5.55 | -2.26 | 3.29 | 43.2 | -0.9 |
| OSQ3 | -5.45 | -2.25 | 3.21 | 46.4 | -0.9 |
| OSQ4 | -5.47 | -2.21 | 3.26 | 44.3 | -1.1 |
| OSQ5 | -6.49 | -3.64 | 2.85 | 40.9 | -1.8 |
| SSQ1 | -5.67 | -2.48 | 3.19 | 42.3 | -0.5 |
| SSQ2 | -5.54 | -2.36 | 3.18 | 38.4 | -0.7 |
| SSQ3 | -5.44 | -2.29 | 3.14 | 37.2 | -0.6 |
| SSQ4 | -5.48 | -2.34 | 3.14 | 38.4 | -0.8 |
| SSQ5 | -6.42 | -3.66 | 2.76 | 38.2 | -1.6 |

[a]Experimental $\gamma$ values from reference 10

shown in Supplementary Data, Table S3). It is observed that the major transition in all the molecules is due to the transition of electron from HOMO to LUMO which contributes more than 90%. The energy levels of the orbitals HOMO and LUMO for SQ1 are -5.72 eV and -2.31 eV, respectively. From this orbital energies, it is noticed that HOMO-LUMO gap (HLG) reduced by 0.03 eV for SQ2 in comparison with SQ1 (the energies of HOMO and LUMO for SQ2 were -5.55 eV and -2.26 eV). In case of molecule SQ3, the energies of HOMO and LUMO orbitals are -5.76 eV and -2.31 eV, respectively and having HLG of 3.45 eV.

These results show that, there is no significant change in HLG by the introduction of electron donating group at ortho/ para position of phenyl ring from the parent molecule SQ1. A significant change in the HOMO-LUMO orbital energies and HLG are observed for SQ5. The HOMO, LUMO and HLG energies for SQ5 are -6.62 eV, -3.59 eV and 3.03 eV, respectively. These results indicate that the lowest HLG for SQ5 is due to more stabilization of HOMO and LUMO levels. Further analyzing the electron density on HOMO and LUMO of SQ1, SQ2, SQ3, SQ4, it is seen that charge transfer occur during electronic transitions from the side phenyl group to central four membered ring along with oxygen/ sulfur attached with central four membered ring. But in case of SQ5, it is observed that, the charge transfer during transition occur from central four membered ring along with oxygens attached to central four membered ring and also to the side phenyl ring (electron withdrawing group attached to the phenyl ring).

With the replacement of oxygen atom with sulfur at central four membered ring having same substituents, results in destabilization of HOMO and stabilization LUMO levels which results in decrease in HLG. For aniline substituted squaraine, HLG for SQ1, OSQ1 and SSQ1 are 3.41 eV, 3.27 eV and 3.19 eV, respectively (Table 4). There is continuous reduction in HOMO-LUMO gap with the replacement of sulfur with oxygen in SQ1→OSQ1→SSQ1. Similar results were observed for all other molecules.

**Charge transfer**

To understand the charge transfer in these molecules, molecules are divided into three groups: 2-heteroatoms (Group I), central 4-membered ring (Group II), and donor substituents (Group III), and electron densities of each group calculated using VMOdes software [43]. The net electron densities of each group have been estimated and tabulated in Table 5. Within series of molecules, Group I and III are acting as electron donors, while central 4-membered ring i.e. Group II acts as acceptor. For SQ1, net electron densities of Group I, Group II and Group III are -23.2e, 35.9e and -12.6e, respectively. From the electron densities, it is clear that charge transfer is from heteroatoms (Group-I) and substituted side groups (Group-III) to the central 4-membered acceptor ring (Group-II). For SQ5, the donation is from only heteroatoms (Group-I, -25.0e) and both Group-II and III are accepting electron densities (shown in Table 5). It clearly shows that introduction of nitro group at phenyl ring result in transfer of charge from Group I to Group II and III due to which there is overall red shift in absorption for nitro group series molecules as shown in Table 2. The similar types of trends are followed for other series of molecules (OSQ5 and SSQ5) except OSQ1 and OSQ2 where Group-III also acts as acceptor (shows acceptance of 5.4e and 1.2e for OSQ1 and OSQ2, respectively).

**Diradicaloid character**

Diradicaloid character (DRC) can be calculated by various methods. According to Wirz, if the energy gap between singlet and triplet is around 2 to 24 kcal mol$^{-1}$, the molecule is said to be diradicaloid[44]. From the literature, it is known that, squaraines with C-C bonding are biradicaloid molecules whereas; squaraines with C-N bonding are non-biradicaloid character[21]. Similar trends were obtained when one or both oxygen atoms are replaced by sulfur atom on central four membered ring. From Table 4, all the molecules have singlet-triplet gap ($E_{S-T}$) around 40 kcal mol$^{-1}$. Hence these molecules can be considered as non-biradicaloid molecules. DRC can also calculated by using occupation numbers method given by Nakano et al.[45]:

$$DC = \left(1 - \frac{2S_i}{1+S_i^2}\right) \times 100 \quad \ldots (1)$$

where, $S_i$ is the orbital overlap between corresponding occupied and unoccupied orbitals (HOMO – i and LUMO + i) and can be determined by using occupation numbers ($n_i$) of unrestricted formalism (UHF) of natural orbitals, expressed as:

$$S_i = n_{HOMO-i} - n_{LUMO+i} \quad \ldots (2)$$

The estimated result using UHF method also indicates non-biradicaloid character for all these molecules (Table 4).

**Second hyperpolarizability (⟨γ⟩)**

The average second hyperpolarizability values, ⟨γ⟩ obtained for all the molecules using various DFT functionals i.e. B3LYP, PBE0, M06, M062X, BHandHLYP, CAM-B3LYP and ωB97XD, with 6-311+G(d,p) basis set based on the B3LYP/6-311+G(d,p) optimized geometries. It is seen that the calculated ⟨γ⟩ values using B3LYP functional are in good agreement with the experimentally available ⟨γ⟩ values for SQ molecules and are shown in Table 4 (⟨γ⟩ values obtained using other functionals are shown in

Table 5 — Charge transfer (in electron unit) from ground state to excited state of SQ, SSQ, and OSQ series of molecules obtained at B3LYP/6-311+G(d,p) level

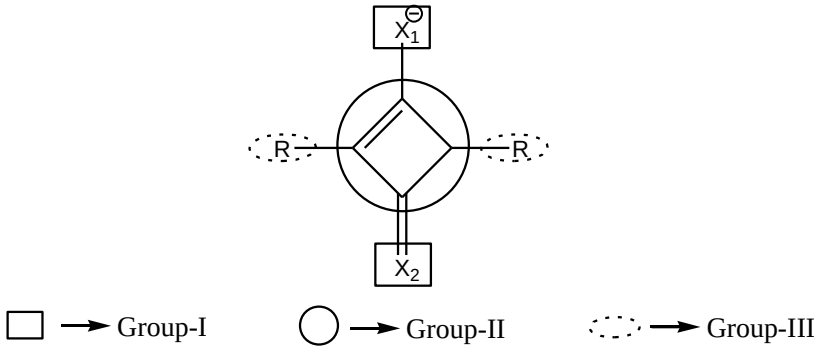


| Molecule | | Group-I (X1 & X2) | Gain/Loss | Group-II (C1-C4) | Gain/Loss | Group-III (R) | Gain/Loss |
|---|---|---|---|---|---|---|---|
| SQ1 | HOMO | 23.3 | -23.2 | 17.5 | 35.9 | 59.2 | -12.6 |
| | LUMO | 0.1 | | 53.4 | | 46.6 | |
| SQ2 | HOMO | 21.5 | -21.4 | 16.1 | 36.8 | 60.5 | -15.1 |
| | LUMO | 0.1 | | 51.3 | | 48.6 | |
| SQ3 | HOMO | 17.5 | -17.4 | 13.9 | 37.4 | 68.6 | -20.0 |
| | LUMO | 0.1 | | 51.3 | | 48.6 | |
| SQ4 | HOMO | 18.2 | -18.1 | 13.6 | 40.2 | 68.1 | -21.9 |
| | LUMO | 0.1 | | 53.8 | | 46.2 | |
| SQ5 | HOMO | 25.0 | -25.0 | 19.1 | 14.3 | 55.9 | 10.7 |
| | LUMO | 0.0 | | 33.4 | | 66.6 | |
| OSQ1 | HOMO | 42.8 | -42.8 | 15.7 | 37.4 | 41.5 | 5.4 |
| | LUMO | 0.0 | | 53.1 | | 46.9 | |
| OSQ2 | HOMO | 39.6 | -39.6 | 14.5 | 38.2 | 44.5 | 1.2 |
| | LUMO | 0.0 | | 52.7 | | 45.7 | |
| OSQ3 | HOMO | 39.6 | -17.4 | 14.8 | 37.4 | 43.1 | -20.0 |
| | LUMO | 0.0 | | 50.5 | | 48.8 | |
| OSQ4 | HOMO | 33.3 | -18.1 | 12.4 | 40.2 | 54.3 | -21.9 |
| | LUMO | 0.0 | | 53.4 | | 46.6 | |
| OSQ5 | HOMO | 46.6 | -46.0 | 17.4 | 14.3 | 36.0 | 29.7 |
| | LUMO | 0.0 | | 34.3 | | 65.7 | |
| SSQ1 | HOMO | 53.4 | -23.2 | 12.8 | 35.9 | 33.8 | -12.6 |
| | LUMO | 20.7 | | 54.4 | | 24.9 | |
| SSQ2 | HOMO | 49.8 | -21.4 | 12.0 | 36.8 | 38.2 | -15.1 |
| | LUMO | 27.1 | | 54.6 | | 18.2 | |
| SSQ3 | HOMO | 47.1 | -7.5 | 11.7 | 42.1 | 41.2 | -34.6 |
| | LUMO | 39.6 | | 53.8 | | 6.6 | |
| SSQ4 | HOMO | 42.5 | -7.3 | 10.5 | 44.7 | 47.0 | -37.4 |
| | LUMO | 35.2 | | 55.2 | | 9.6 | |
| SSQ5 | HOMO | 58.0 | -57.7 | 14.0 | 20.2 | 28.0 | 37.5 |
| | LUMO | 0.3 | | 34.2 | | 65.5 | |

Supplementary Data, Table S4). All the molecules showed $\langle\gamma\rangle$ of the order of $10^{-34}$ esu. Similarly, $\langle\gamma\rangle$ values calculated for other series molecules i.e. OSQ and SSQ. SQ1, OSQ1 and SSQ1 molecules are having $\langle\gamma\rangle$ value of $2\times10^{-34}$, $0.5\times10^{-34}$ and $0.6\times10^{-34}$ esu, respectively (Table 4 and Supplementary Data, Fig. S2). It is also observed that the introduction of electron withdrawing group (i.e. nitro group) at the phenyl ring shows enhancement in the $\langle\gamma\rangle$ value.

## Conclusions

Fifteen molecules of visible absorbing C-N bonding, symmetrical squaraine dyes are studied by using DFT and TDDFT methods. It has been found that, for SQ and SSQ molecules anti-configuration is more stable than syn-configuration. OSQ molecules prefer to have syn-arrangement towards the oxygen atom i.e. OSQ-c is more stable than anti-configuration. For all three sets of molecules there is

an increase in absorption, as we change the squaraine from unsubstituted squaraine to substituted squaraine, however red shift is maximum in case of SQ5 (~56 nm), OSQ (~50 nm) and SSQ (~78 nm). For the same substituents there is almost 70 nm red shift in absorption with addition of two sulfur atoms in place of oxygen atom. The replacement of oxygen atom at central four membered ring with heteroatom (X=S) in squaraine dyes results in bathochromic shifts (either in OSQ or SSQ molecules to their parent SQ molecules). This noticeable red shift in absorption is due to greater donor ability of sulfur atom and its less electronegativity than oxygen atom. High value of singlet-triplet energy gap in all SQ, OSQ, SSQ molecules indicates that these are non-biradicaloid molecules. Further, the calculated $\langle\gamma\rangle$ values are in the order of $10^{-34}$ esu for all the molecules.

## Supplementary Data

Supplementary Data associated with this article are available in the electronic form at http://nopr.niscair.res.in/jinfo/ijca/IJCA_60A(03)370-377_SupplData.pdf.

## Acknowledgment

PC thanks CSIR- New Delhi, India for financial support [No. 02(0339)/18/EMR-II].

## References

1 Treibs A & Jacob K, *Angew Chem Int Ed*, 4 (1965) 694.
2 Ohno M, Yamamoto Y, Shirasaki Y & Eguch S, *J Chem Soc Perkin Trans*, 2 (1993) 263.
3 Maahs G & Hegenberg P, *Angew Chem Int Ed*, 5 (1966) 88.
4 Meier H, Petermann R & Gerold, *Chem Commun*, 11 (1999) 977.
*5* Sreejith S, Carol P, Chithra P & Ajayaghosh A, *J Mater Chem*, 18 (2008) 264.
6 Ohsedo Y, Saruhashi K & Watanabe H, *Dyes Pigm*, 122 (2015) 134.
7 Sprenger H E & Ziegenbein W, *Angew Chem Int Ed*, 5 (1966) 894.
8 Schmidt A H, *Synthesis*, 12 (1980) 961.
9 Park S Y, Jun K & Oh S W, *B Korean Chem Soc*, 26 (2005) 428.
10 Prabhakar C, Bhanuprakash K, Rao V J, Balamuralikrishna M & Rao D N, *J Phys Chem C*, 114 (2010) 6077.
11 Lee S, Rao B A & Son Y A, *Sens Actuators B*, 210 (2015) 519.
12 Silva C E, Diniz R, Rodrigues B L & Oliveira de L F C, *J Mol Struct*, 831 (2007) 187.
13 Tripathi A, Promila & Prabhakar C, *J Phys Org Chem*, 30 (2017) e3673.
14 Promila, Tripathi A & Prabhakar C, *Indian J Chem*, 57A (2018) 1121.
15 Anna K K, Marta Z B, Dorota C, Przemysław K & Halina K, *J Photochem Photobiol A*, 318 (2016) 77.
16 Conceicao D S, Ferreira D P, Graca V C, Silva C R, Santos P F & Ferreira L F V, *Tetrahedron*, 71 (2015) 967.
17 Maltase V, Cospito S, Beneduci A, Simone B C D, Russo N, Chidichimo G & Janssen R A J, *Chem Eur J*, 22 (2016) 10179.
18 Meier H & Petermann R, *Helv Chim Acta*, 87 (2004) 1109.
19 Chandrasekaran Y, Dutta G K, Kanth R B & Patil S, *Dyes Pigm*, 83 (2009) 162.
20 Ajayaghosh A, *Acc Chem Res*, 38 (2005) 449.
21 Pandey S S, Morimoto T, Fujikawa N & Hayase S, *Sol Energy Mat Sol Cells*, 159 (2017) 625.
22 Law K Y, *Chem Rev*, 93 (1993) 449.
23 Law K Y & Bailey F C, *J Org Chem*, 57 (1992) 3278.
24 Fabian J, Nakazumi H & Matsuoka M, *Chem Rev*, 92 (1992) 1197.
25 Mustroph H, Stollenwerk M & Bressau V, *Angew Chem Int Ed*, 45 (2006) 2016.
26 Li Z, Jin Z H, Kasatani K, Okamoto H & Takenaka S, *Jpn J Appl Phys*, 44 (2005) 4956.
27 Xiao J, Liu Z, Zhang X, Wu W, Ren T, Lv B, Jiang L, Wang X, Chen H, Su W & Zhao J, *Dyes Pigm*, 112 (2015) 176.
28 Yum J H, Walter P, Huber S, Rentsch D, Geiger T, Nuesch F, Angelis F D, Gratzel M & Nazeeruddin M K, *J Am Chem Soc*, 129 (2007) 10320.
29 Karpenko I A, Collot M, Richert L, Valencia C, Villa P, Mely Y, Hibert M, Bonnet D & Klymchenko A S, *J Am Chem Soc*, 137 (2015) 405.
30 Langhals H, *Angew Chem Int Ed*, 42 (2003) 4286.
31 Meier H & Dullweber U, *J Org Chem*, 62 (1997) 4821.
32 Meier H & Dullweber U, *Tetrahedron Lett*, 37 (1996) 1191.
33 Bigelow R W & Freund H J, *Chem Phys*, 107 (1986) 159.
34 Law K Y, *J Phys Chem*, 915 (1987) 184.
35 Prabhakar C, Yesudas K, Chaitanya G K, Sitha S, Bhanuprakash K & Rao V J, *J Phys Chem A*, 109 (2005) 8604.
36 Puyad A L, Prabhakar C, Yesudas K, Bhanuprakash K & Rao V J, *J Mol Struc- Theochem*, 904 (2009) 1.
37 Puyad A L, Chaitanya G K, Prabhakar C & Bhanuprakash K, *J Mol Mod*, 19 (2013) 275.
38 Lee C, Yang W & Parr R G, *Phys Rev B*, 37 (1988) 785.
39 Becke A D, *J Chem Phys*, 98 (1993) 5648.
40 *Gaussian 16, Rev. E.01*, Gaussian, Inc., Wallingford, CT (2016).
41 Bredas J L, Adant C, Tackx P, Petersoons A & Pierce B M, *Chem Rev*, 94 (1994) 243.
42 Kurdyukov V V, Tolmachev A I, Dekhtyar M L, Vlasenko Y G & Chernega A N, *J Phys Org Chem*, 28 (2015) 452.
43 Nemykin V N & Basu P, *VMOdes Program, Revision A 7.1*, Department of Chemistry, Duquesne University, Pittsburgh, PA 2001, 2003.
44 Wirz J, *Pure Appl Chem*, 56 (1984) 1289.
*45* Nakano M, Nitta T, Yamaguchi K, Champagne B & Botek E, *J Phys Chem A*, 108 (2004) 4105.
46 Jurek K, Kabatc J & Kostrzewska K, *Dyes Pigm*, 133 (2016) 273.